

# NEW MEASUREMENTS OF THE PROTON STRUCTURE FUNCTIONS $F_2$ AND $F_L$ AT LOW $Q^2$ AT HERA

V. LENDERMANN

*Kirchhoff-Institut für Physik, Universität Heidelberg,  
Im Neuenheimer Feld 227, 69120 Heidelberg, Germany  
E-mail: victor@mail.desy.de*

New results of the measurements of the proton structure functions  $F_2$  and  $F_L$  at low  $Q^2$  at HERA are presented. The measurements cover mainly the transition region of  $Q^2 \sim 1 \text{ GeV}^2$  between the domains of deep inelastic scattering and quasi-real photoproduction. For the  $F_2$  measurements radiative events are employed by H1, in order to extend the covered range of Bjorken  $x$  towards higher values. The results are used to study the  $x$  dependence of  $F_2(x, Q^2)$  in the non-perturbative regime. Furthermore, the first direct  $F_L$  extraction performed by ZEUS using radiative events and a new “shape method” of the  $F_L$  extraction with higher precision by H1 are discussed.

## 1 Introduction

Measurements of lepton-nucleon deep inelastic scattering (DIS) have played a crucial role for our understanding of proton structure and for the development of Quantum Chromodynamics (QCD). In the last decades much progress was made in extending the kinematic range of measurements in terms of the Bjorken variable  $x$  and the modulus of four-momentum transfer squared  $Q^2$ . In particular, the H1 and ZEUS experiments at the HERA  $ep$  collider have shown that the  $Q^2$  evolution of the proton structure function  $F_2(x, Q^2)$  is well described by perturbative QCD (pQCD) throughout a wide range in  $x$  and  $Q^2$ . However, at small  $Q^2 \lesssim 1 \text{ GeV}^2$  the transition takes place into a region in which quark confinement effects dominate, pQCD is no longer applicable, and, instead of the quarkonic degrees of freedom, the hadronic ones have to be considered. The data in this region are described by phenomenological models.

Special experimental techniques are necessary in order to access this region at HERA, as the detector acceptance in standard inclusive measurements restricts the angular range of the detected scattered electrons<sup>a</sup>

such that only events at  $Q^2 > 1 \text{ GeV}^2$  can be recorded. One ansatz is to use a special detector mounted close to the outgoing electron beam direction<sup>1</sup> which gives access to very low  $Q^2$  values. An alternative approach is to perform dedicated runs with the interaction vertex shifted in the proton beam direction. Preliminary results of a new measurement at  $0.35 < Q^2 < 3.5 \text{ GeV}^2$  and  $7 \cdot 10^{-6} < x < 2 \cdot 10^{-3}$  were recently presented by the H1 collaboration<sup>2</sup>. The data were taken at HERA in 2000 in a run with the interaction vertex shifted by 70 cm.

In this paper an extension<sup>3</sup> of that measurement towards higher  $x$  values is discussed, which makes use of events with hard photons emitted nearly collinear to the electron beam, so called Initial State Radiation (ISR) data. Furthermore, a complimentary approach to access higher  $x$  is presented<sup>4</sup>, in which events with wide angle bremsstrahlung, referred to as QED Compton (QECD) events, are used. Afterwards a first direct extraction of the longitudinal structure function of protons  $F_L$  from ISR data by the ZEUS collaboration<sup>5</sup> is discussed. Finally, a new “shape method” of indirect  $F_L$  determination with increased precision, as employed by H1<sup>6</sup>, is described.

<sup>a</sup>The generic name “electron” is used to denote both

electrons and positrons.

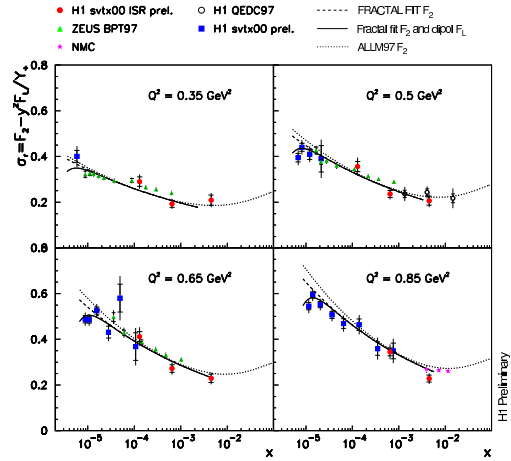


Figure 1. Reduced cross section measurements at  $Q^2 < 1 \text{ GeV}^2$  by H1 (preliminary), ZEUS and NMC. The lines represent various phenomenological fits.

## 2 Cross Section Measurement Using ISR Data

Contrary to the previous HERA measurements<sup>8,9,5</sup>, the emitted photon is not tagged explicitly in the new H1 ISR analysis<sup>3</sup>. Instead, its energy is inferred from the missing longitudinal momentum. As in the other recent H1 low  $Q^2$  measurements, the Backward Silicon Tracker is used to identify the scattered electron and to reduce the contamination by neutral particle backgrounds.

The new data cover the region  $0.35 \lesssim Q^2 \lesssim 0.85 \text{ GeV}^2$  and  $10^{-4} \lesssim x \lesssim 5 \cdot 10^{-3}$ . In Fig. 1 the reduced cross section

$$\sigma_r = \frac{Q^4 x}{2\pi\alpha^2} \frac{d^2\sigma}{dxdQ^2} = F_2(x, Q^2) - \frac{y^2}{Y_+} F_L(x, Q^2) \quad (1)$$

with the inelasticity  $y = Q^2/(xs)$  and  $Y_+ = 1 + (1 - y)^2$ , for the new data is compared with the standard analysis of H1 shifted vertex data as well as with data from the ZEUS beam pipe tracker<sup>1</sup>, from the H1 QEDC measurement<sup>4</sup> and from NMC<sup>10</sup>. The new data are in agreement with the other measurements. The predictions of the extrapolated Fractal model fit<sup>11</sup> and the ALLM97 parametrisation<sup>12</sup> are also displayed. All pre-

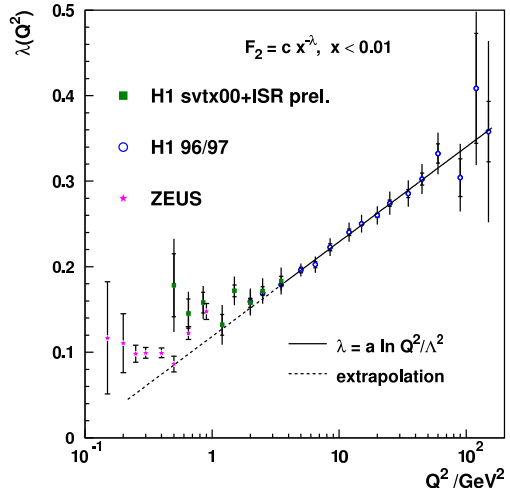


Figure 2. Selected HERA results of the  $\lambda$  extraction from low  $x$  data.

dictions are in good agreement with the data.

Recently the H1 collaboration presented<sup>2</sup> an extraction of the parameter  $\lambda$  from fits of the form  $F_2 = c(Q^2) \cdot x^{-\lambda(Q^2)}$ . This parameter quantifies the rise of  $F_2$  towards low  $x$  at fixed  $Q^2$ . The new analysis allows an improved extraction of  $\lambda$  from the H1 data. The results, obtained by fitting the present data at fixed  $Q^2$  values together with the previous shifted vertex measurements, are shown in Fig. 2. The new measurements confirm the change in behaviour of  $\lambda$  from a logarithmic dependence on  $Q^2$  at large  $Q^2$  to a weaker dependence compatible with reaching a constant consistent with soft pomeron intercept as  $Q^2 \rightarrow 0$ . The change takes place at distance scales of  $\sim 0.3 \text{ fm}$  and can be interpreted as being related to a transition from partonic to hadronic degrees of freedom.

## 3 $F_2$ Measurement Using QED Compton Scattering

QED Compton events are radiative  $ep$  events characterised by low virtuality of the exchanged photon and sizeable virtuality of the exchanged electron. The experimental signature is an approximately back-to-back az-

imuthal configuration of the outgoing electron and photon. In this configuration their transverse momenta nearly balance such that it is possible to reconstruct the event kinematics for very small values of  $Q^2$ .

The first  $F_2$  measurement in inelastic QEDC scattering is performed by H1<sup>4</sup> using data from the 1997 standard running period. A prominent background to inelastic QEDC scattering arises from inclusive DIS events in which one particle from the hadronic final state (typically a  $\pi^0$ ) fakes the outgoing photon. At high  $y$ , where the hadronic final state lies mostly in the backward region, this process dominates the QEDC signature, hampering a clean QEDC event selection. For this reason the measurement is restricted to relatively low  $y$  values:  $y < 0.0062$ .

At so low  $y$  the variables  $x$  and  $y$  cannot be determined solely from the measured electron and photon four-momenta, since their resolution deteriorates as  $1/y$ . Hence for the kinematic reconstruction the  $\Sigma$ -method is employed, which also uses information from the hadronic final state. As low  $y$  values correspond to small polar angles of the final state hadrons, one of the main challenges for the analysis is the correct reconstruction of the total momentum of the hadronic final state in light of the losses beyond the forward acceptance of the detector. This necessitates a good simulation of hadronisation processes at low  $Q^2$  and low invariant masses  $W$ . The simulation of the hadronic final state down to the resonance region is performed using the SOPHIA program<sup>13</sup>.

The  $F_2$  values measured in QED Compton scattering are shown in Fig. 3 as a function of  $x$  at fixed  $Q^2$  and are compared with other HERA and fixed target data. The QEDC analysis extends the kinematic range of HERA measurements at low  $Q^2$  towards higher  $x$  values, thus complementing standard inclusive and shifted vertex measurements. The measurement is consistent with the results of fixed target experiments in the

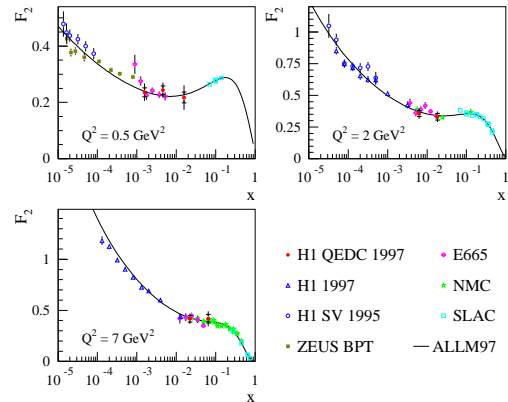


Figure 3.  $F_2$  measurements from QED Compton scattering by H1 (closed circles), compared with other measurements at HERA and fixed target experiments. The solid line depicts the ALLM97 parametrisation.

overlapping region. The data are also well described by the ALLM97 parametrisation<sup>12</sup>.

#### 4 $F_L$ Extraction

The inclusive  $ep$  cross section is sensitive to the contribution of longitudinally polarised photons at large  $y$  only (see eq. 1). A direct determination of  $F_L$  would require cross section values measured at different  $y$  values for the same  $x$  and  $Q^2$ . This can be achieved, e.g., by performing special runs at lower proton beam energies. Such runs are a part of the HERA II physics program.

Alternatively, events with tagged Initial State Radiation can be employed, as first presented by ZEUS<sup>5</sup>. The ISR process is interpreted as the inclusive  $ep$  scattering at a reduced electron beam energy. The emitted photon is detected in the luminosity monitor. The result of the ZEUS analysis of the data taken during 1996 and 1997 running periods are shown in Fig. 4. Much more statistics is required in order to achieve a sufficient accuracy of the  $F_L$  measurement in ISR.

A higher accuracy is achieved using indirect methods of  $F_L$  extraction, which are based on the analysis of the reduced cross

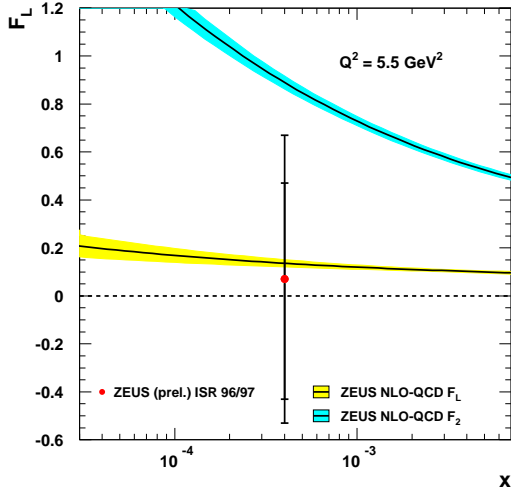


Figure 4. ZEUS ISR result for  $F_L$  plotted for  $x = 4 \cdot 10^{-4}$  and  $Q^2 = 5.5 \text{ GeV}^2$ . The yellow band shows the prediction for  $F_L$  from the ZEUS NLO QCD fit. The light blue band shows the prediction for  $F_2$ , which is the maximum possible value of  $F_L$ .

section behaviour at high  $y$  values. The data of the minimum bias 1999<sup>7</sup> and shifted vertex 2000<sup>2</sup> runs are used by H1<sup>6</sup> to extract  $F_L$  by two methods: the derivative method and the new “shape method”.

The new method employs the shape of  $\sigma_r$  in a given  $Q^2$  bin. The shape is driven at high  $y$  by the kinematic factor  $y^2/Y_+$  (eq. 1), and to a lesser extent by  $F_L(x, Q^2)$  which is considered to be constant:  $F_L = F_L(Q^2)$ .

Based on the analysis of the rise of  $F_2$  towards low  $x$ , the reduced cross section is fitted by:

$$\sigma_{r,\text{fit}} = cx^{-\lambda} - \frac{y^2}{Y_+} F_L , \quad (2)$$

and  $F_L$  is determined from the fit for different  $Q^2$  bins. The errors obtained turn out to be significantly smaller than those from the derivative method.

The results for a fixed invariant mass of the hadronic final state,  $W = 276 \text{ GeV}$ , are presented in Fig. 5, in which an overview of all current H1 data in the  $Q^2$  range  $0.75 \leq Q^2 \leq 700 \text{ GeV}^2$  is given. The data are compared with higher order QCD fits. The H1 data

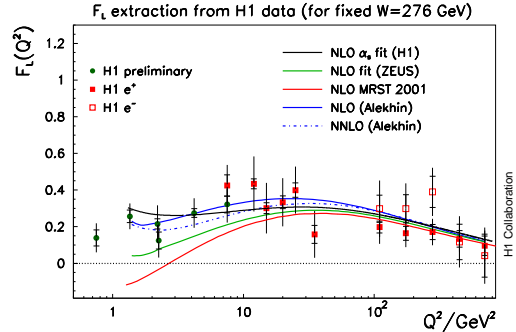


Figure 5.  $Q^2$  dependence of  $F_L(x, Q^2)$  at fixed  $W = 276 \text{ GeV}$ , summarizing the H1 data. The lines show various NLO and NNLO QCD fits.

favour a positive, not small  $F_L$  at low  $Q^2$ . A negative  $F_L$  is experimentally ruled out.

## References

1. J. Breitweg *et al.* [ZEUS Collaboration], *Phys. Lett. B* **487**, 53 (2000).
2. H1 Collaboration, Contributed paper to EPS 2003, Aachen, Abstract **082**.
3. H1 Collaboration, Contributed paper to ICHEP 2004, Beijing, Abstract **5-0170**.
4. A. Aktas *et al.* [H1 Collaboration], *Phys. Lett. B* **598**, 159 (2004).
5. ZEUS Collaboration, Contributed paper to EPS 2003, Aachen, Abstract **502**.
6. H1 Collaboration, Contributed paper to ICHEP 2004, Beijing, Abstract **5-0161**.
7. H1 Collaboration, Contributed paper to EPS 2001, Budapest, Abstract **799**.
8. T. Ahmed *et al.* [H1 Collaboration], *Z. Phys. C* **66**, 529 (1995).
9. M. Derrick *et al.* [ZEUS Collaboration], *Z. Phys. C* **69**, 607 (1996).
10. M. Arneodo *et al.* [New Muon Collaboration], *Nucl. Phys. B* **483**, 3 (1997).
11. T. Laštovička: *Eur. Phys. J. C* **24**, 529 (2002).
12. H. Abramowicz and A. Levy, DESY-97-251, hep-ph/9712415.
13. A. Mücke *et al.*, *Comput. Phys. Commun.* **124**, 290 (2000).